Biosensors and Bioelectronics 29 (2011) 60–65

Contents lists available at ScienceDirect

Biosensors and Bioelectronics

journal homepage: www.elsevier.com/locate/bios

Au-nanocluster emission based glucose sensing

A.M.P. Hussain [a], S.N. Sarangi [b], J.A. Kesarwani [c], S.N. Sahu [b,*]

[a] Department of Physics, Cotton College, Guwahati, Assam 781001, India
[b] Institute of Physics, Bhubaneswar 751005, India
[c] Ayush Hospital, Bhoi Nagar, Achyarya Vihar, Bhubaneswar 751022, India

ARTICLE INFO

Article history:
Received 10 May 2011
Received in revised form 25 July 2011
Accepted 27 July 2011
Available online 3 August 2011

Keywords:
Gold cluster
Fluorescence
Glucose biosensor
Optical absorption

ABSTRACT

Fabrication of a glucose biosensor based on Au-cluster emission quenching in the UV region is reported. The glucose biosensor is highly sensitive to β-D-glucose in 2.5–25.0 mM range as confirmed from a linear calibration plot between Au-cluster colloid emission intensity as a function of β-D-glucose concentration. The interaction of β-D-glucose with L-cysteine capped Au cluster colloids has been confirmed from their Fourier transformed infrared spectroscopy (FTIR) measurements. It has been found that the biomolecules present in the serum such as ascorbic and uric acids, proteins and peptides do not interfere and affect in glucose estimation as confirmed from their absorption and fluorescence (FL) emission measurements. Practical utility of this sensor based on FL quenching method has been demonstrated by estimating the glucose level in human serum that includes diabetes and the data were found to be comparable or more accurate than those of the pathological data obtained from a local hospital. In addition, this biosensor is useful to detect glucose level over a wide range with sensor response time of the order of nano to picoseconds that is emission lifetime of Au clusters.

1. Introduction

Noble metal nanoparticles (NPs) such as Au and Ag have shown to exhibit size- and shape-dependent surface plasmon resonance (SPR) absorption and emission properties and dimensional similarities with biomolecules. Hence, integration of biomolecules with metallic NPs have led to applications in the areas of biosensor (Anker et al., 2008), biology, biomedical (Huang et al., 2009) and molecular probe for light-based imaging (Rayavarapu et al., 2007). Au NPs with large surface to volume ratio are highly reactive contrary to the bulk-Au. In addition, the Au NPs can immobilize biomolecules by a simple electrostatic interaction which can cause a change in dielectric constant of Au NPs microenvironment which would result in the SPR absorption and emission peak shift along with the change of emission intensities (Parui et al., 2004). These specific optical properties can be used to detect biomolecules such as glucose in serum samples and also estimate its concentrations. Detection and estimation of glucose level in human serum, specifically with diabetes is very important and has been widely investigated. Estimation of blood glucose level by routine glucose biosensors (Heller and Feldman, 2008; Ansari et al., 2004; Tang et al., 2004a; Huang et al., 2005) have been a challenging task due to their inherent problems of large sensor response time (Tang et al., 2004b), small calibration range (Huang et al., 2005), durability (Park et al., 2003) and interferences (Huang et al., 2005; Yonzon et al., 2004; Faradji et al., 2005; Safavi et al., 2009) present in serum. Furthermore, the sensor durability is limited due to the enzyme that catalyzes the oxidation requires replenishment (Park et al., 2003). Glucose biosensors based on amperometric (Safavi et al., 2009; Wang et al., 2006) methods, nanowires/nanotubes (Barone et al., 2004; Rong et al., 2007; Salimi et al., 2004), microchip electrophoresis (Maeda et al., 2007), enzyme field effect transistor (Dzyadevich et al., 1999), spectrophotometry (Zhu et al., 1997), surface enhanced Raman scattering (Yonzon et al., 2004) and diffraction (Asher et al., 2003) techniques have been reported in the literature but are limited to their glucose detection range and interference effects related to bovine serum albumin (BSA) (Yonzon et al., 2004), peptides (Faradji et al., 2005) and uric and ascorbic acids (Safavi et al., 2009). Fluorescence (FL) resonance energy transfer (FRET) between a FL donor and an acceptor leading to glucose induced changes (Pickup et al., 2005) is a promising technique and features a physiological detection range between 16 μM and 1.0 mM (Ballerstadt and Schultz, 2000; Tang et al., 2008) whereas the normal human blood glucose level lies between 3 and 7 mM range and biomolecules similar to glucose is expected to interfere in glucose estimation which can give false positives (Ballerstadt and Schultz, 2000). Specifically, for Au dot glucose sensor (Huang et al., 2009; Shiang et al., 2009), the emission from Au dot appearing at 522 nm is of very low intensity. In addition, the red shift of the surface plasmon resonance (SPR) emission from the SPR absorption of Au NPs as high as 147 nm is difficult to understand compared to standard results (Jain et al., 2006; Sarangi et al., 2009). Aslam et al. (2004a,b)

* Corresponding author. Tel.: +91 674 2306407; fax: +91 674 2300142.
E-mail address: sahu@iopb.res.in (S.N. Sahu).

0956-5663/$ – see front matter © 2011 Elsevier B.V. All rights reserved.
doi:10.1016/j.bios.2011.07.066

reported a dextran coated Au NP SPR absorbance based glucose sensor where the calibration was drawn with out using the SPR absorption peak at 520 nm. On the contrary, a long wavelength tailing part at 650 nm of the absorption spectrum was used to detect glucose but without considering the interference effects. Although Aslam et al. (2004b) could detect glucose, based on luminescence intensity enhancement of Ag NPs but the mechanism for such enhancement is less understood and neither the glucose concentration nor the reason for luminescence enhancement are being reported. Recent glucose detection techniques are based on monitoring higher glucose concentration detection with concanavalin A (conA) aggregated dextran coated Au NPs (Aslam et al., 2004a) (size, 10 nm) SPR absorption at 650 nm wavelength and surface enhanced FL for mono- or polysaccharide detection using boronic acid capped Ag NPs (Aslam et al., 2004b) SPR emission. Although these techniques are sensitive to glucose detection, but have not considered (i) the linearity in sensor response, (ii) application to human serum and (iii) the interference effect. Au NPs are known to have large negative real and small imaginary dielectric constant (Anker et al., 2008), large scattering cross-section (Lee et al., 2007) and are sensitive to the local refractive index change, hence, the SPR absorption and luminescence peak positions are shifted with reduced intensity when anchored with organic ligands with higher refractive indices (Anker et al., 2008). However, bare Au NPs have little affinity to analytes (glucose) (Anker et al., 2008), hence, usually Au NPs are capped with an organic ligand which apart from passivating the surface sites, can also provide stability. The biocompatible organic ligand, L-cysteine in contrast to TOPO (Jain et al., 2006), apart from fabricating smallest Au NPs with better passivation (Sarangi et al., 2009), can also strongly interact with β-D-glucose to form the Au cluster-L-cysteine–β-D-glucose complex which neither require any external power source as in electrochemical glucose biosensor nor require any donor and acceptor as in FRET (Ballerstadt and Schultz, 2000; Tang et al., 2008). The present work reports the fabrication of a highly stable glucose biosensor based on FL emission quenching of Au cluster colloids with out major interference effects and its subsequent use in the estimation of glucose level in human serum samples that include diabetes. This sensor is expected to be useful for the fast quantitative determination of glucose level in human serum, being more robust, easier to use with highly accurate data.

2. Materials and methods

2.1. Synthesis of Au-NPs (Au-cluster) colloid

Preparation Au-NP colloids has been reported elsewhere (Sarangi et al., 2009). In short, highly stable monodispersed Au-NPs colloids were prepared by the reduction of $AuCl_4$ (0.5 M) with $NaBH_4$ (0.01 M) in the presence of L-cysteine (2.0 mM). 25 ml aqueous solution of 2.0 M L-cysteine was prepared at room temperature. Stock solution of 0.05 M $HAuCl_4$ was prepared with double distilled deionized water. Then, 250 μl of 0.05 M $HAuCl_4$ was added to 25 ml of 2.0 mM L-cysteine and stirred for 30 min. To this solution, 350 μl of 0.01 M $NaBH_4$ was added under constant stirring for 2.0 h. The product is a L-cysteine capped Au-NP colloids which were washed and centrifuged to remove any residue chemical precursors. The high resolution transmission electron microscope (HRTEM) image of Au-NP colloids exhibited monocrystalline character with size as 2.0 nm and had very narrow size distribution (Sarangi et al., 2009). These L-cysteine capped Au NPs exhibited absorption maxima, λ_{max} and FL emission at 365 and 382 nm, respectively. Absence of SPR absorption at 520 nm wavelength, appearance of λ_{max} and FL in UV region has led us to predict Au NPs could be the clusters of eight atom Au because of its stable structure (Sarangi et al., 2009). Indeed, these Au NP colloids are confirmed to be the Au_8 clusters (Rath et al., 2010). Hence onward, we refer the Au NPs as Au clusters (Supplementary text, S1) throughout this article.

2.2. Synthesis of Au-cluster β-D-glucose complex and sensor calibration

Aqueous solution of β-D-glucose (beta form of dextrose, mol. wt. 180.16 g and 99% pure) was prepared in the concentration range 0.25–40.0 mM. 20 μl freshly prepared β-D-glucose solution was added to 2.5 ml L-cysteine capped Au clusters colloids for each concentration of β-D-glucose in the range 0.25–40.0 mM. The mixture was then stabilized for 5.0 min. The interaction of β-D-glucose with L-cysteine capped Au cluster is studied by FTIR (Saga 370, Thermonicolet, USA) measurement. This solution was then used to calibrate the glucose sensor by fluorescence (FL) quenching method. The sensor calibration was performed after mixing 1.5 ml of the freshly prepared β-D-glucose solution in the range of 0.25–40.0 mM with 2.5 ml of as prepared water dispersed Au cluster colloids and the FL as well as absorption were recorded. The performance of the FL quenching based biosensor was evaluated routinely and the glucose levels estimated were compared with those of the clinical data.

2.3. Preparation of human serum-Au-cluster complex

To estimate the glucose level, the human serum samples were obtained from Ayush Hospital, Bhubaneswar with prior approval from the hospital review committee as well as with the consent from the patients. The serum sample was then mixed with the Au clusters in similar ratio by volume to that of the β-D-glucose used to calibrate the sensor. For example, 20 μl of serum sample was mixed with 2.500 ml of Au cluster colloid solution. For each experiment, the total volume was kept at 2.520 ml which is same as used in the calibration. Human serum samples were collected by a pathologist from different donors that include diabetic patients. The pathologist has followed a standard hospital procedure to extract serum from blood and estimated the glucose level by a spectroscopic method in the hospital. A residue of the same serum sample was used to estimate the glucose level by the FL emission quenching method. The serum samples, received from the hospital were stored in a freezer at 4 °C.

2.4. Fluorescence (FL) and absorbance measurements

The FL and the absorption spectra were collected at room temperature. The FL emission spectra of Au cluster, Au cluster with β-D-glucose and Au cluster with serum were carried out using an Oriel (USA) Photoluminescence set up consisting of Hg–Xe lamp excitation source, a single monochromator, a second monochromator with SPECTRACQ2 (Jobin Yvon, France) module to allow different wavelengths to detect by a PMT detector and a PC. The UV–vis absorption spectra relative to de-ionized water were recorded using a dual beam spectrophotometer (Shimazu, Japan) in the wavelength range 200–700 nm. The emission spectra were collected under 250 nm wavelength excitation. The FL emission intensities are the normalized intensities collected with out changing the slit width and gain of the monochromator for each of the samples.

3. Results and discussion

The FL behavior of the Au cluster and Au-cluster-β-D-glucose complex were recorded at room temperature under $\lambda = 250$ nm wavelength excitation to achieve intense FL because of the appearance of Au cluster absorption maxima at 365 nm (Sarangi et al.,

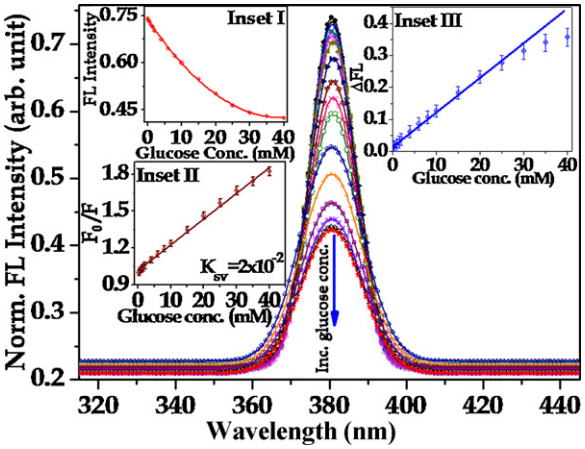

Fig. 1. FL spectra of Au-cluster–β-D-glucose complex with different concentration of β-D-glucose (0.0 mM–40.0 mM), inset I – FL intensity as a function of β-D-glucose concentration, inset II – Stern–Volmer plot showing a dynamic quenching and inset III is the calibration plot.

2009). Shown in Fig. 1 is the spontaneous Au cluster emission spectra with increased β-D-glucose concentration (top, first spectrum is the reference). The FL intensities of Au cluster depict a consistent decrease in intensity with increasing β-D-glucose concentrations but with out any change in spectral shape or position. The reduction in intensity is due to increased dielectric constant and change in refractive index (Anker et al., 2008; Huang et al., 2009; Rayavarapu et al., 2007; Parui et al., 2004) of the surrounding medium of Au cluster as a result of interaction with β-D-glucose to form a complex with the organic ligand, L-cysteine. This result is in contrast to the fluorescence enhanced glucose sensor (Aslam et al., 2004b) based on a different surface chemistry Ag NP–saccharide interaction. Unlike the FL quenching based glucose biosensors developed by Aslam and Perez-Luna (2004) using Au NPs, the effect of absorption and dilution influencing the FL yield are not considered here. This is because 20 nm Au colloids used by Aslam and Perez-Luna (2004) is expected to yield less intense SPR emission and the stability of the FL with the increased Au NP concentration would be reached after a certain period of time in contrast to a stable FL of Au cluster colloids (for a period of 5 months) in the present work. In addition, the durability of the present glucose sensor is better than those of electrochemical glucose sensors (Ansari et al., 2004; Park et al., 2003; Yonzon et al., 2004) whose enzymes that catalyze the oxidation require replenishment. As the cluster emission lifetime is of the order of few nano- to picoseconds, the present glucose sensor response time should be of the same order in contrast to those of electrochemical glucose sensors (Ansari et al., 2004; Tang et al., 2004a). The plot of Au cluster FL intensity as a function of β-D-glucose concentration (Fig. 1, inset I) shows a linear decrease of FL from 2 mM to 15 mM β-D-glucose. Above 15 mM, it is non-linear and tends to saturate after 30 mM. The linearity in the Stern–Volmer plot (Fig. 1, inset II) suggests the dynamic quenching which increases with the increase of the quencher concentration (Lakowicz, 1999). The change in FL intensity, ΔFL with β-D-glucose concentration, known as the calibration plot, is shown in Fig. 1 (inset III) which is linear from 2.0 mM to 25 mM. This calibration curve is best fitted using a regression line equation given by

$$y = a + bx \tag{1}$$

where

$$b = \frac{\sum_{i=1}^{n} x_i y_i - n\bar{x}\bar{y}}{\sum_{i=1}^{n} x_i{}^2 - n\bar{x}^2} \tag{2}$$

and $a = \bar{y} - b\bar{x}$

The obtained values are $\bar{x} = 12.15$, $\bar{y} = 0.145$, $a = 0.023$, $b = 0.01$ and the regression line equation is $y = 0.023 + 0.01x$.

The correlation coefficient (r) is calculated from the standard relation given by

$$r = \frac{n\sum_{i=1}^{n} x_i y_i - \sum_{i=1}^{n} x_i \sum_{i=1}^{n} y_i}{\sqrt{\left(\sum_{i=1}^{n} x_i{}^2 - \left(\sum_{i=1}^{n} x_i\right)^2\right)\left(n\sum_{i=1}^{n} y_i{}^2 - \left(\sum_{i=1}^{n} y_i\right)^2\right)}} \tag{3}$$

where n is the total number of data points, x_i are the x values and y_i are the y values.

The value of r obtained as 0.997 which indicates a strong positive relationship of the calibration. The plot shows linear change in intensity in 2.5–25 mM β-D-glucose range. The resolution of the glucose sensor expressed by the change in FL to the change in glucose concentration ($\Delta FL/\Delta GC$) is better than any glucose sensors working in this range because of the steeper calibration curve.

The FL intensity is sensitive even to a very small concentration of β-D-glucose, 0.25 mM, which could not be observed in electrochemical glucose sensors based on current–voltage measurement giving a mean error of 2.3 mM (Garjonyte and Malinauskas, 1999). The interaction of β-D-glucose with L-cysteine capped Au cluster is confirmed from the FTIR measurements. Specifically, the ring deformation vibrational absorption band at 586 cm^{-1} is found to be shifted with reduced intensity which confirms to a covalent linkage of β-D-glucose with L-cysteine capped Au cluster (supplementary text S2).

Ascorbic and uric acids present in human serum often influence the glucose biosensor performance (Safavi et al., 2009). Attempts have been made to identify such interferences using Au cluster colloids. No absorption from either ascorbic or uric acids with Au cluster colloids have been detected in the wavelength range of interest (supplementary text S3). Similarly, no FL emission from either ascorbic or uric acids with Au cluster colloids could be detected in the wavelength range of interest which can interfere with Au cluster emission (Supplementary text, S3). Other possible interfering species such as BSA and peptide present in the serum too can influence the glucose level estimation. Hence, the absorption spectra of six representative serum samples that include diabetes are shown in Fig. 2(a). The strong absorption band at 280 nm due to BSA (Faradji et al., 2005; Zhuang et al., 2008) whose intensities vary arbitrarily with different serum samples although the peak positions do not change. On the other hand, the low intense c-peptide absorption peak at 413 nm (Faradji et al., 2005) nm do change in a definite fashion presumably the c-peptide amount become more with increasing glucose level in the serum. The increasing c-peptide content in the serum samples suggest to higher insulin secretion from pancreas and indicates that the blood samples collected from different patients have early stages of diabetics (type II diabetes). At a later stage, the secretion of insulin will recede to yield lesser c-peptide in the blood and the patient is expected to succumb to retinopathy (Sari and Balci, 2005). Note that samples S3 and S6 in Fig. 2(a) show higher c-peptide content. The absorption spectra of Au cluster, Au-cluster + BSA and bare BSA are shown in Fig. 2(b). The BSA absorption peak at 280 nm is far apart from Au cluster absorption peak position, hence, do not interfere in absorption measurement. The same 280 nm absorption peak is also obtained from the bare serum sample (Fig. 2(a)). As the c-peptide peak at 413 nm is also far apart from Au cluster absorption peak at 365 nm, c-peptide too do not interfere in glucose absorption measurement. As our motivation is to estimate glucose level by FL quenching method, the FL spectra under 250 nm wavelength excitation for Aucluster, Au-cluster + BSA, bare BSA and atypical serum samples are shown in Fig. 3.

The FL spectra of the serum sample exhibited only one broad emission peak at 344 nm from BSA but there is no emission from

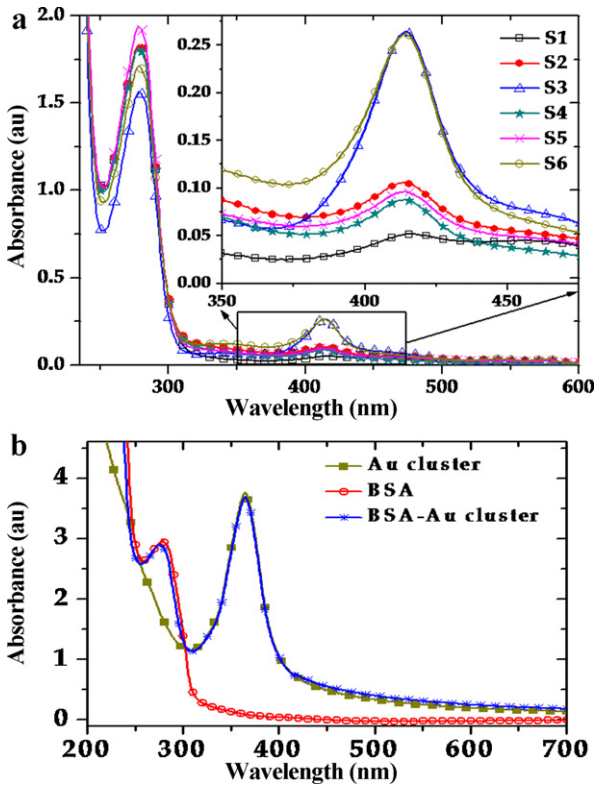

Fig. 2. (a) Absorption spectra of serum sample showing the presence of BSA and c-peptide peaks. In set: expanded view of absorption peak of c-peptide showing higher absorption intensity in serum samples (samples S3 and S6 from diabetic patients). (b) Absorption spectra of commercial BSA, Au-cluster and BSA with Au cluster.

the C-peptide owing to its insulating nature. The FL spectra of BSA and BSA with Au cluster colloids also exhibited the broad FL peak at 344 nm due to BSA alone. The spectral shape, intensity and line width of the FL peak due to Au cluster appearing at 382 nm are found to be unchanged. We conclude here that BSA and C-peptide as interfering species do not affect the glucose sensor performance. Other interfering biological species like maltose, lactose, fructose, galactose, mannose, etc. carbohydrates may also get attached to the Au clusters, but the total concentration of glucose in human blood is 100-fold higher than all other carbohydrates (Shiang et al., 2009). Thus, the interferences from the carbohydrates being very small, the effects are ignored (Shiang et al., 2009).

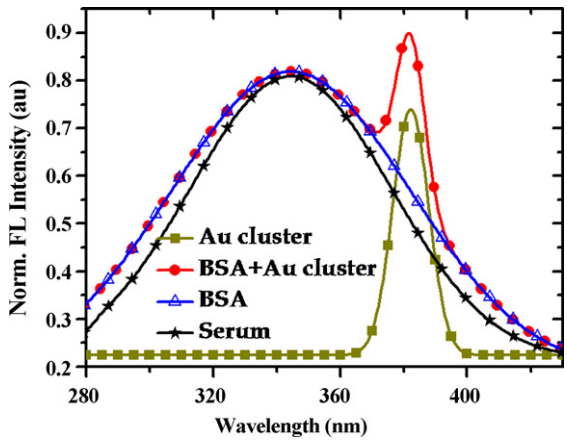

Fig. 3. FL spectra of serum sample, Au cluster colloids, Au cluster colloids with BSA and bare BSA.

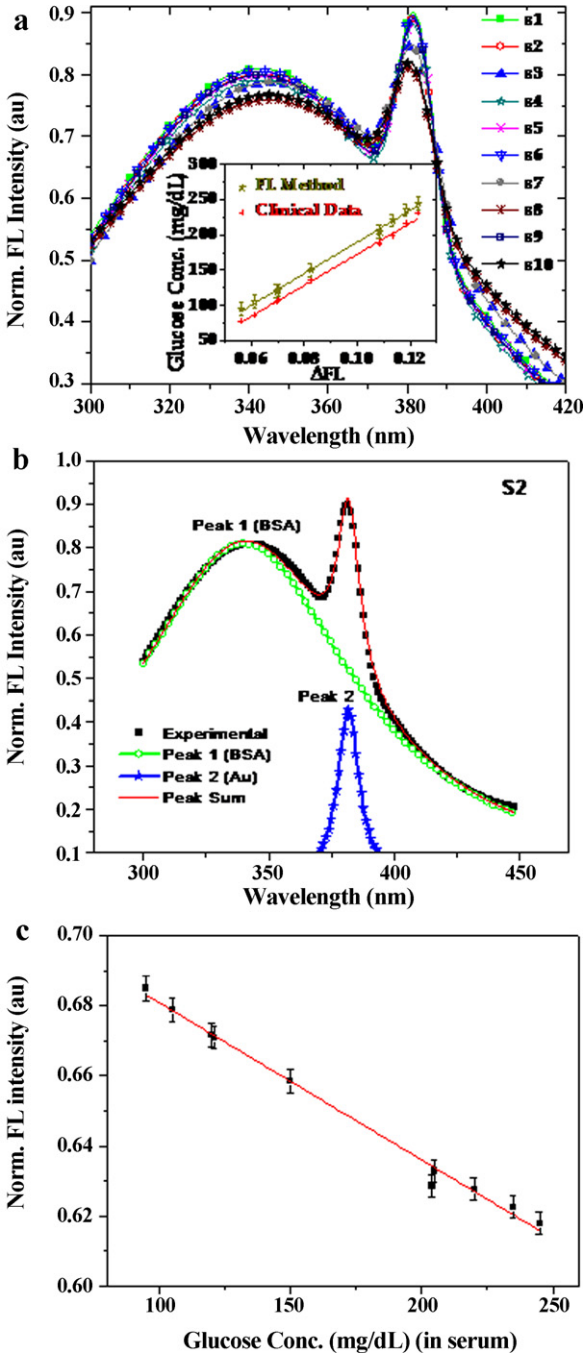

Fig. 4. (a) FL spectra of Au cluster-serum complex, inset: plots showing the glucose levels estimated by the FL quenching method to those of clinical data. (b) Experimental curve fitting of the serum sample, S2. (c) The calculated dose responsive curve (FL as a function of glucose level in different serum samples).

Fig. 4(a) shows the FL emission of Au cluster with serum sample obtained from different donors. Narrow Gaussian FL peaks corresponding to different glucose levels in the serum samples appear at 382 nm whose intensities decrease with increasing glucose level without any change in spectral position or shape similar to Fig. 1. This suggests that the glucose in the serum has interacted with Au cluster colloids and change in FL intensity is a function of glucose concentration in different serum samples. In addition, a broad FL peak at 344 appear which corresponds to BSA in the serum samples whose intensities too decreases showing a similar trend to those of the FL quenched glucose spectra (Fig. 1). Here too, the FL spectral shape and peak position of BSA do not change. A similar

Table 1
Glucose concentration estimated by FL quenching method and by standard pathological data from local hospital.

Sample no.	Glucose concentration (mg/dL)	
	Present method (FL quenching)	Pathological data from hospital
S1	122 ± 2.8	107
S2	95 ± 3.1	78
S3	204 ± 4.7	187
S4	105 ± 2.6	86
S5	121 ± 2.9	105
S6	220 ± 3.7	198
S7	235 ± 3.1	215
S8	150 ± 2.5	135
S9	245 ± 3.5	230
S10	205 ± 3.2	188

broad FL peak positioned at 344 nm is also observed for commercial BSA with Au cluster (Fig. 3) colloids. This means that both BSA and glucose in the serum samples together interact with L-cysteine capped Au clusters as discussed earlier. Hence, BSA concentration in the serum sample can also be estimated by the present FL quenching method by constructing a calibration curve (similar to Fig. 1(inset III)) between BSA and Au cluster FL quenching. However, the present work is more focused on glucose level estimation in the serum samples. So, no efforts have been made to estimate the BSA concentration. Note that FL peak of BSA appearing at 344 nm is less by about 38 nm from Au cluster FL peak and does not affect the FL peak position or shape of Au cluster emission. Hence, BSA should not interfere in glucose estimation. As both BSA and glucose in the serum samples contribute to the FL, the FL intensity of the serum sample should be the summation of two spectrums and the resultant intensity should be higher than Au cluster FL intensity alone. Hence, from Fig. 4(a), the FL intensity (for least amount of glucose level) of Au cluster peak is greater and off the scale when compared to Fig. 1. The actual intensity can be calculated by curve fitting procedure shown in Fig. 4(b) as a representative case (the least quenched spectrum of Fig. 4(a), S2). Note that the actual FL intensity of glucose is now less than Au cluster FL peak alone. All the FL spectra of the serum sample with Au cluster colloids are deconvoluted and the FL intensities of glucose in the serum sample were calculated.

Using the calibration curve (Fig. 1, inset III), the glucose concentrations were estimated and presented in Table 1. The estimated glucose levels from different serum samples obtained from different donors including diabetes and the pathological data obtained from the local hospital (Table 1) are plotted against the change in FL intensities (ΔFL), shown in Fig. 4(a) (inset). The estimated glucose levels present in different serum samples are comparable to those obtained from the local hospital. The linear regression analysis between experimentally observed ΔFL (present work) and glucose concentration for serum samples (Fig. 4(a)) is carried out in a similar manner as Eqs. (1)–(3). The parameter obtained are: $\bar{x} = 0.099$, $\bar{y} = 191.545$, $a = -51.60$, $b = 2445.331$, $y = 2445.331x - 51.609$ and $r = 0.996$. Our estimated glucose levels are found to be on an average of 15% higher than the clinical data (Table 1) because of the non-interference from interfering species as discussed earlier. Fig. 4(c) shows the dose-responsive curve of human serum samples with Au cluster colloids. The FL intensity exhibited consistent linear decrease in the dose–response curve with increasing glucose concentration in the serum samples. The linear regression analysis of Fig. 4(c) has also been carried out in a similar manner as in Eqs. (1)–(3) and the parameters obtained are: $\bar{x} = 170$, $\bar{y} = 0.649$, $a = 0.726$, $b = -0.0004$, $y = 0.026 - 0.0004x$, $r = -0.996$. From the above discussion, it is evident that the glucose level estimation in the present work is fairly accurate and particularly helpful for diabetic patients. In general, with existing glucose biosensors, the estimated blood glucose levels often give lower values when the interferences and protein precipitation in the neonatal blood are not considered (Wang et al., 2006; Salimi et al., 2004).

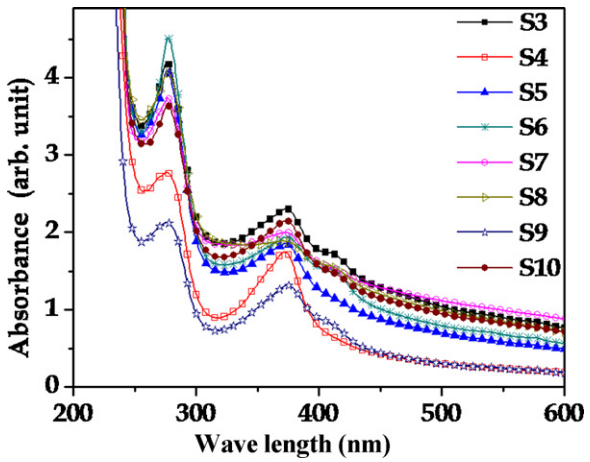

Fig. 5. Representative UV–vis absorption spectra of Au cluster. Colloids with different serum samples obtained from different patients.

The absorption spectra of Au cluster colloids with serum (Fig. 5) (representative spectra are presented to avoid overlapping) identify three distinct absorption peaks at 280 nm, 360 nm and 413 nm, respectively. The highest occupied molecular orbital (HOMO)–lowest un-occupied molecular orbital (LUMO) transition from Au cluster at 365 nm (Sarangi et al., 2009) is blue shifted by 5 nm after interaction with glucose molecule due to the change in dielectrics and the transition peak at 360 nm do not change its spectral shape, position and width even though the serum samples are from different donors. The same 5.0 nm blue shift of Au cluster absorption is also observed when the absorption spectra of Au cluster colloids with β-D-glucose are recorded (supplementary text S4). It can be noted that the absorption spectra of Au-cluster with different concentrations of β-D-glucose exhibit a linear absorption quenching, from where a calibration curve for spectrophotometric glucose estimation can be plotted but the presence of random amount of C-peptide level absorption peak at 413 nm (Faradji et al., 2005) interfere with this calibration which would result erroneous glucose estimation. The absorption peak at 280 nm corresponds to BSA present in the serum (Zhuang et al., 2008) is also confirmed from Au-cluster-BSA absorption measurements. Here too, the peak position (280 nm) and spectral shape (Fig. 5) are unchanged where as the peak intensities have no correlations with the glucose level.

4. Conclusion

In conclusion, we have demonstrated a new approach for the fabrication of highly sensitive, wider range and stable (Au cluster colloids are stable at least up to 5 months) glucose biosensor based on FL (interband radiative transition from LUMO to HOMO states) emission quenching of Au cluster colloids for detection and estimation of glucose level in the serum samples. As the inter band radiative transition lifetime of Au cluster colloids is of the order of nano to picoseconds, the response time of glucose biosensors based on FL quenching should be much shorter than the electrochemical or spectrophotometric glucose sensors reported. The Au cluster colloids are able to eliminate potential interferences such as BSA, C-peptide, uric and ascorbic acids and carbohydrates present in the serum. For a luminescence quenching based sensors, the detection range will depend upon the luminescence intensity. The high luminescence intensity of the Au clusters colloids, provide a

wider calibration range enabling to measure higher glucose levels with high resolution and glucose level as low as 0.25 mM in the serum sample can be detected using the present Au cluster emission quenching method.

Acknowledgements

Authors would like to acknowledge Dr. C.S. Mohapatra and the pathology staff of Ayush Hospital, Bhubaneswar. Dr. U.K. Khadenga of Aditya Care Hospital, Bhubaneswar is acknowledged for fruitful discussion.

Appendix A. Supplementary data

Supplementary data associated with this article can be found, in the online version, at doi:10.1016/j.bios.2011.07.066.

References

Anker, J.N., Hall, W.P., Lyandres, O., Shah, N.C., Zhao, J., Van Duyne, R.P., 2008. Nat. Mater. 7, 442–453.
Ansari, R.R., Böckle, S., Rovati, L., 2004. J. Biomed. Opt. 9, 103–115.
Asher, S.A., Alexeev, V.L., Goponenko, A.V., Sharma, A.C., Lednev, I.K., Wilcox, C.S., Finegold, D.N., 2003. J. Am. Chem. Soc. 125, 3322–3329.
Aslam, K., Lakowicz, J.R., Goddes, C.D., 2004a. Anal. Biochem. 330, 145–155.
Aslam, K., Lakowicz, J.R., Goddes, C.D., 2004b. J. Fluoresc. 14, 391–400.
Aslam, K., Perez-Luna, V.H., 2004. J. Fluoresc. 14, 401–405.
Ballerstadt, R., Schultz, J.S., 2000. Anal. Chem. 72, 4185–4192.
Barone, P.W., Baik, S., Heller, D.A., Strano, M.S., 2004. Nat. Mater. 4, 86–92.
Dzyadevich, S.V., Korpan, Y.I., Arkhipova, V.N., Alesina, M.Y., Martlet, C., El'Skaya, A.V., Soldatkin, A.P., 1999. Biosen. Bioelectron. 14, 283–287.
Faradji, R.N., Monroy, K., Cure, P., Froud, T., Baidal, D., Pileggi, A., Messinger, S., Ricordi, C., Alejandro, R., 2005. Transplant. Proc. 37, 3433–3434.
Garjonyte, R., Malinauskas, A., 1999. Sens. Actuat. B 56, 85–92.
Heller, A., Feldman, B., 2008. Chem. Rev. 108, 2482–2505.
Huang, X., Neretina, S., El-Sayed, M.A., 2009. Adv. Mater. 21, 4880–4910.
Huang, Y., Zheng, W., Xiao, H., Li, G., 2005. Biosen. Bioelectron. 21, 817–821.
Jain, P.K., Lee, K.S., El-Sayed, I.H., El-Sayed, M.A., 2006. J. Phys. Chem. B 110, 7238–7248.
Lakowicz, J.R., 1999. Principles of Fluorescence Spectroscopy, 2nd ed. Kluwer Academic, NY.
Lee, J., Hernandez, P., Lee, J., Govorov, A.O., Kotov, N.A., 2007. Nat. Mater. 6, 291–295.
Maeda, E., Kataoka, M., Hino, M., Kajimoto, K., Kaji, N., Tokeshi, M., Kido Shinohara, J.Y., Baba, Y., 2007. Electrophoresis 28, 2927–2933.
Park, S., Chung, T.D., Kim, H.C., 2003. Anal. Chem. 75, 3046–3049.
Parui, P.P., Nath, D.N., Chowdhury, M., 2004. Chem. Phys. Lett. 396, 329–334.
Pickup, J.C., Hussain, F., Evans, N.D., Rolinski, O.J., DBirch, D.J.S., 2005. Biosen. Bioelectron. 20, 2555–2565.
Rath, S., Nozaki, S., Palagin, D., Matulis, V., Ivashkevich, O., Maki, S., 2010. Appl. Phys. Lett. 97, 053105–053105.
Rayavarapu, R.G., Petersen, W., Ungureanu, C., Post, J.N., Van Leeuwen, T.G., Manohar, S., 2007. Int. J. Biomed. Imaging, doi:10.1155/2007/29817, Article ID 29817.
Rong, L.-Q., Yang, C., Qian, Q.-Y., Xia, X.-H., 2007. Talanta 72, 819–824.
Safavi, A., Maleki, N., Farjami, E., 2009. Biosen. Bioelectron. 24, 1655–1660.
Salimi, A., Compton, R.G., Hallaj, R., 2004. Anal. Biochem. 333, 49–56.
Sarangi, S.N., Hussain, A.M.P., Sahu, S.N., 2009. Appl. Phys. Lett. 95, 073109–073111.
Sari,.R., Balci, M.K., 2005. J. Natl. Med. Assoc. 97, 1113–1118.
Shiang, Y.C., Huang, C.C., Chang, T., 2009. Chem. Commun., 3437–3439.
Tang, B., Cao, L., Xu, K., Zhuo, L., Ge, J., Li, Q., Yu, L., 2008. Chem. Eur. J. 14, 3637–3644.
Tang, H., Chen, J., Yao, S., Nie, L., Deng, G., Kuang, Y., 2004a. Anal. Biochem. 331, 89–97.
Tang, H., Chem, J., Yao, S., Nie, L., Deng, G., Kuang, Y., 2004b. Anal. Biochem. 331, 89–97.
Wang, J.X., Sun, X.W., Wei, A., Lei, Y., Cai, X.P., Li, C.M., Dong, Z.L., 2006. Appl. Phys. Lett. 88, 233106–233108.
Yonzon, C.R., Haynes, C.L., Zhang, X., Walsh Jr., J.T., Van Duyne, R.P., 2004. Anal. Chem. 76, 78–85.
Zhuang, Z., Su, X., Yuan, H., Sun, Q., Xiao, D., Choi, M.M.F., 2008. Analyst 133, 126–132.
Zhu, M., Huang, X.M., Shen, H.X., 1997. Anal. Chim. Acta 349, 165–170.